

Reducing the Quantum Many-electron Problem to Two Electrons with Machine Learning

LeeAnn M. Sager-Smith¹ and David A. Mazziotti^{1,*}

¹*Department of Chemistry and The James Franck Institute,
The University of Chicago, Chicago, IL 60637 USA*

(Dated: Submitted July 6, 2022; Revised August 19, 2022)

Abstract. An outstanding challenge in chemical computation is the many-electron problem where computational methodologies scale prohibitively with system size. The energy of any molecule can be expressed as a weighted sum of the energies of two-electron wave functions that are computable from only a two-electron calculation. Despite the physical elegance of this extended “aufbau” principle, the determination of the distribution of weights—geminal occupations—for general molecular systems has remained elusive. Here we introduce a new paradigm for electronic structure where approximate geminal-occupation distributions are “learned” via a convolutional neural network. We show that the neural network learns the N -representability conditions, constraints on the distribution for it to represent an N -electron system. By training on hydrocarbon isomers with only 2-7 carbon atoms, we are able to predict the energies for isomers of octane as well as hydrocarbons with 8-15 carbons. The present work demonstrates that machine learning can be used to reduce the many-electron problem to an effective two-electron problem, opening new opportunities for accurately predicting electronic structure.

Introduction

For any molecular system, the Schrödinger equation can, *in theory*, be solved exactly using a full configuration interaction (FCI) calculation [1–3] with a complete basis set; however, *in practice*, the computational complexity of such an exact approach grows factorially with system size [3], making molecular systems with more than a few dozen electrons intractable. Over time, many approximate methodologies have been introduced in an attempt to obtain “good enough” solutions to the electronic Schrödinger equation that predict energies within chemical accuracy (~ 1 kcal/mol).

Hartree-Fock theory—a mean-field approach—yields reasonable results for a wide array of molecular systems containing up to a few hundred atoms [2]; however, it fails in molecules in which the motions of electrons are significantly correlated. Techniques which more-accurately capture correlation energy such as many-body perturbation theory, coupled cluster theory, complete active-space self-consistent field theory, and others remain computationally expensive for large system sizes [2, 4]. The so-called many-electron problem—whereby the cost of highly-accurate *ab initio* computational methodologies scales in a prohibitive manner with system size—is hence an outstanding challenge in chemical computations.

Machine learning may enable us to circumvent this problem by allowing us to use information about smaller molecules to treat correlation in larger systems at a reduced cost [5]. It has been used to learn the energies of various molecular structures [6–9], new functionals for density functional theory (DFT) [10–12], inverse problems in electronic structure theory [13, 14], and even the many-body wave function of one-dimensional spin systems [15]. However, these areas are in their early stages and have yet to demonstrate definite success in decreasing the degree of scaling with system size.

In this *Article* we introduce a new paradigm for utilizing machine learning in quantum chemistry in which we reduce the quantum many-electron problem to a more tractable, bet-

ter scaling two-electron problem. As originally proposed by Bopp [16, 17], the energy of a molecule of arbitrary size can be expressed without approximation as a weighted sum of the energies of two-electron wave functions, known as geminals. However, despite its physical significance as an extension of the “aufbau” principle, the distribution of weights—geminal occupations—has remained elusive. Here, we show that the geminal-occupation distribution can be learned with machine learning. We use a convolutional neural network (CNN) to learn an effective temperature in a Boltzmann-like distribution for the geminal occupations. The effective temperature—or correlation temperature—is inversely related to the electron correlation. The neural network, we demonstrate, learns the N -representability of the distribution—the representability of the distribution by an N -electron system [18–21], which appears as a nonzero temperature. The scheme can be viewed as a two-electron reduced density matrix (2-RDM) theory as the geminal occupations are an integral part of the 2-RDM. A schematic of the machine learning algorithm for predicting molecular energies is shown in Fig. 1.

We apply the machine learning algorithm to hydrocarbon systems. Specifically, by training a convolutional neural network on all isomers of ethane through heptane, we predict the correlation temperatures—and hence molecular energies—of all of the isomers of octane as well as all straight-chained hydrocarbons from octane through pentadecane. We find that this RDM-based machine learning method accurately recovers the correlation energy for larger hydrocarbon systems, with the N -representability conditions being learned by the CNN framework. Our approach—which scales as $O[n^6]$ —improves upon the exponential scaling of traditional configuration-interaction calculations, foreshadowing the potential utility of this machine-learning reduced density matrix approach to the determination of accurate molecular energies. While polynomial-scaling levels of theory such as Coupled Cluster with Single and Double Excitations (CCSD) can be used to treat weakly-correlated systems such as the hydrocarbons presented in this manuscript,

if trained on appropriate molecular data, our convolutional network approach may be capable of accurately recovering correlation energy for more highly-correlated systems.

Results and Discussion

Theory. Central to our modern understanding of chemistry is the concept of the molecular orbital. Any molecule’s electronic structure can be readily understood in terms of its molecular orbitals which are filled from lowest-in-energy to highest-in-energy by the Pauli exclusion principle. When electrons of a molecule become strongly correlated, however, the orbital picture with unit filling of the lowest orbitals breaks down. Because electronic interactions are at most pairwise, the orbital picture can in principle be replaced by an exact two-electron (geminal) picture, which is derivable from 2-RDM theory.

The ground- or excited-state energy of any atom or molecule is expressible as an exact functional of the 2-RDM (2D) [16, 18, 19, 22–59]

$$E = \int {}^2\hat{K} {}^2D(\bar{1}\bar{2}; 12)d1d2 \quad (1)$$

where ${}^2\hat{K}$ is the reduced Hamiltonian operator

$${}^2\hat{K} = -\frac{N}{2} \left(\frac{\hat{p}_1^2}{2m} + \frac{\hat{p}_2^2}{2m} + \sum_k \frac{Z_k}{r_{1k}} + \sum_k \frac{Z_k}{r_{2k}} \right) + \frac{N(N-1)}{2} \frac{1}{r_{12}}. \quad (2)$$

In a finite orbital basis set, the operators are expressible as a reduced Hamiltonian matrix. Diagonalization of this reduced Hamiltonian matrix yields a set of eigenvalues and eigenvectors (or geminals). In the basis set of geminals, the Hamiltonian is a diagonal matrix consisting of its eigenvalues, the 2-RDM has a non-negative diagonal elements which we denote by p_i , and energy is the sum over the geminal eigenvalues of the Hamiltonian matrix ϵ_i weighted by the non-negative geminal occupations p_i :

$$E = \sum_i p_i \epsilon_i. \quad (3)$$

By this transformation we express the energy as a functional of the eigenvalues of the reduced Hamiltonian ϵ_i , which are readily computed at the cost of the two-electron calculation, and the unknown geminal occupations p_i (see Fig. 2).

The German chemist Bopp originally proposed approximating the geminal occupation numbers by a Pauli-like filling scheme [16, 17]. He suggested choosing the lowest $N(N-1)/2$ to be equal to one. This approach, while analogous to the filling of orbitals in molecular-orbital theory, generates accurate energies for four-electron atoms and ions but energies for larger molecular systems that are too low. Coleman suggested that the filling of the geminal by two electrons—or the pseudo-particle called a pairon—should follow

a fundamental probability distribution as in statistical mechanics [16]. He proposed a Boltzmann distribution for the geminal occupations based on the geminal energies. While such a distribution is not exact because the pairon pseudo-particles obey neither the Fermi-Dirac or Bose-Einstein particle statistics, there exists a Boltzmann-like distribution given by

$$p_i = \frac{N(N-1)}{Z} e^{-\epsilon_i/kT^*} \quad (4)$$

and parameterized by a specific correlation temperature (T^*) such that the resultant approximate geminal probability distribution allows for the accurate computation of a molecule’s energy according to Eq. (3). However, the ability to determine such a correlation temperature is currently only possible if the geminal energies (ϵ_i) and geminal populations (p_i) are both known.

Here, we train a convolutional neural network (CNN) to predict the correlation temperature for a given molecular system consistent with its ground-state energy. The convolutional neural network is trained on inputs corresponding to both geminal energies—expressed as partition functions given by

$$Z = \sum_i e^{-\epsilon_i/kT} \quad (5)$$

for a variety of temperatures—as well as the computed Hartree-Fock correlation temperature (T_{HF}^*) and with training outputs corresponding to a Δ value representing the difference between the exact (i.e. configuration interaction) correlation temperature and the HF correlation temperature, i.e., $\Delta = T_{EXACT}^* - T_{HF}^*$. For larger molecular systems, we then predict the Δ values by reading in the geminal energies and Hartree-Fock correlation temperatures for those molecules into the trained neural network. These Δ values are then added to the T_{HF}^* s in order to yield the exact correlation temperatures, which allows for the approximation of the geminal probability distributions and hence the molecular energies via Eq. (3).

In general, for two-electron reduced density matrix methodologies, the 2-RDM must be constrained to represent the N -electron wavefunction through application of N -representability constraints [18–21]. Here, if N -representability conditions are not accounted for in our Boltzmann-like machine learning approach, the correlation temperature would be zero, which corresponds to the lowest-energy geminal being fully occupied by all electron pairs. This electronic structure machine learning approach, however, maintains N -representability by learning correlation temperatures from N -representable training data and applying this inherent “learned” N -representability to the testing data.

See the Experimental section at the end of this document for additional details.

Energetic Predictions for Isomers of Octane. For the eight-ten isomers of octane—with molecular geometries obtained

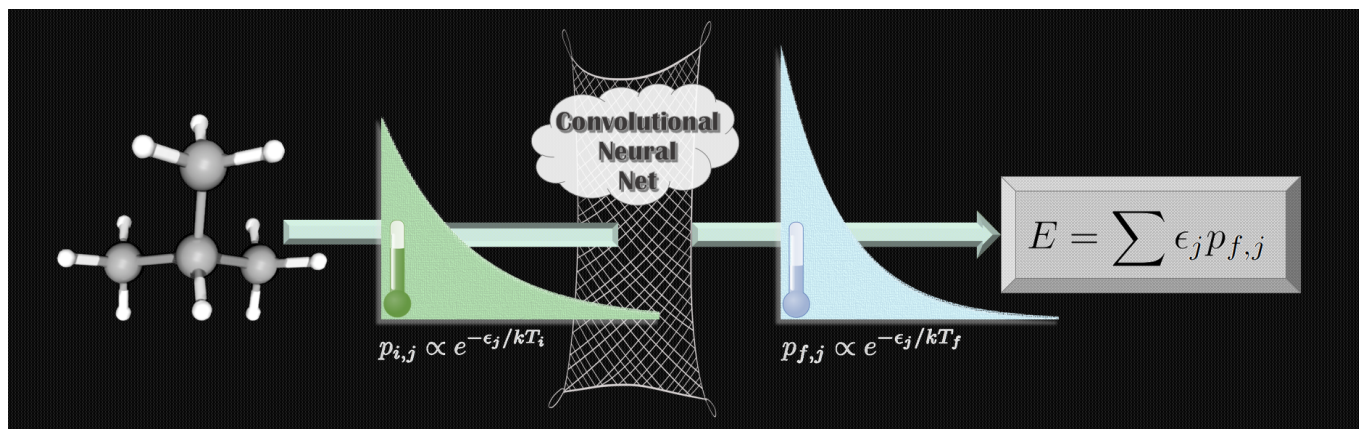


FIG. 1: **Graphic demonstrating algorithm flow.** For a given molecule, a trained convolutional neural network is used to predict the Boltzmann-like correlation temperature (T_f) with the eigenfunctions of the reduced Hamiltonian (ϵ_j) and the Hartree-Fock correlation temperature (T_i) as inputs. The correlation temperature (T_f) allows for the approximation of the geminal populations ($p_{f,j}$) by Eq. (4), which is sufficient for the prediction of the energy by Eq. (3).

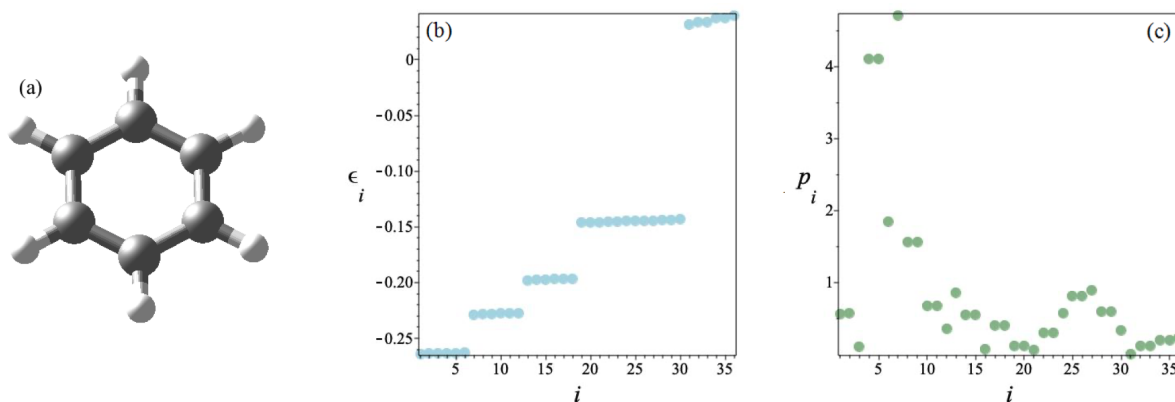


FIG. 2: **Example of geminal energies and probabilities.** For (a) benzene, we can use the (b) geminal energies ϵ_i to learn the (c) geminal probabilities p_i —both of which are computed here from a [$N_e = 6$, $N_o = 6$] complete active-space self-consistent-field (CASSCF) using the minimal Slater-type orbital basis set with six Gaussian primitive functions representing each Slater-type orbital (STO-6G). Knowing both geminal energies and geminal populations is sufficient to determine molecular energies via Eq. (3).

from the PubChem database [60]—, the Hartree-Fock and CASSCF energies are computed using Dunning’s double-zeta (cc-pVDZ) basis set with complete active-space self-consistent-field (CASSCF) calculations employing a [$N_e = 8$, $N_o = 8$] active space. Utilizing a convolutional neural network trained on hydrocarbons ranging from two to seven carbon atoms, the correlation temperature corresponding to the CASSCF energy is predicted for each of the octane isomers and used to compute the predicted CASSCF energies shown in Fig. 3(a). As can be seen from this figure, which shows energy versus isomer identifier, the predicted CASSCF energies (green circles) show good agreement with the actual CASSCF energies (black boxes), vastly improving upon the Hartree-Fock energies (blue diamonds), and hence our predictions capture the correlation energy in a fairly accurate manner.

Additionally, in order to demonstrate the generality of our reduced density matrix approach for “learning” molecular energies, Coupled Cluster Single Double (CCSD) energies are computed for the cc-pVDZ basis for hydrocarbons ranging from two to seven carbon atoms. The corresponding CCSD correlation temperatures are then used to train a convolutional neural net, and the correlation temperature corresponding to the CCSD energy is then predicted for each isomer of octane, with the resultant predicted CCSD energies shown in Fig. 3(b). Similar to the CASSCF energies from Fig. 3(a), the CCSD predicted energies (green circles) demonstrate good agreement with the actual CCSD energies (black boxes) when compared to the Hartree-Fock energies (blue diamonds). Hence, for this second level of theory, our predictions capture correlation energies in a fairly accurate manner. Additional predictions corresponding to CCSD cal-

culations utilizing the STO-6G basis set can be seen in the Supporting Information.

We next explore systems composed of larger hydrocarbons to determine whether such good agreement remains consistent as system size is increased while the training data remains the same.

Energetic Predictions for Large Hydrocarbon. For the eight straight-chained hydrocarbons ranging from octane to pentadecane—with molecular geometries obtained from the PubChem database [60]—, the Hartree-Fock and CASSCF energies are computed using Dunning’s double-zeta (cc-pVDZ) basis set with the CASSCF calculations employing a [$N_e = 8$, $N_o = 8$] active space. Utilizing a convolutional neural network trained on hydrocarbons ranging from two to seven carbon atoms, the correlation temperature corresponding to the CASSCF energy is predicted for each of the octane to pentadecane hydrocarbon isomers and used to compute the predicted CASSCF energies shown in Fig. 4. As can be seen from this figure, which shows energy per carbon versus number of carbons, the predicted CASSCF energies (green circles) show good agreement with the actual CASSCF energies (black boxes), vastly improving upon the Hartree-Fock energies (blue diamonds), and hence our predictions capture the correlation energy in a fairly accurate manner. Although there is a slight increase in the error as system size is increased, it appears to be small enough that the energies of even larger hydrocarbon isomers may be able to be predicted in an accurate manner through use of our convolutional neural network trained on only hydrocarbons with seven or fewer carbon atoms. Similar promising results are obtained for predicting CASSCF energies for octane, nonane, decane, and undecane via a convolutional neural network trained on CASSCF calculations for hydrocarbons with two to seven carbons that utilize a [10,10] active space and the cc-pVTZ basis set as can be seen in the Supporting Information.

Conclusions

In this *Article*, we introduce a new paradigm based on a two-electron, reduced density matrix approach for the utilization of machine learning architecture in the prediction of accurate correlation energies for molecular systems at reduced computational expense. By employing a Boltzmann-like distribution for two-electron geminal populations parameterized by a correlation temperature, we train a convolutional neural network on correlation temperatures corresponding to CASSCF and CCSD calculations for smaller molecular systems in order to predict CASSCF and CCSD correlation temperatures for larger, more computationally-expensive molecular systems and hence obtain predicted CASSCF/CCSD energies. Moreover, the N -representability conditions are inherently maintained by our CNN framework—as evinced by nonzero correlation temperatures. This methodology for the prediction of CASSCF energies scales as $O[n^6]$ with the number of orbitals due to the diagonalization of the reduced Hamilto-

nian, which is an improvement over the exponential scaling of a traditional CASSCF calculation. See the Experimental section for additional comments on computational scaling.

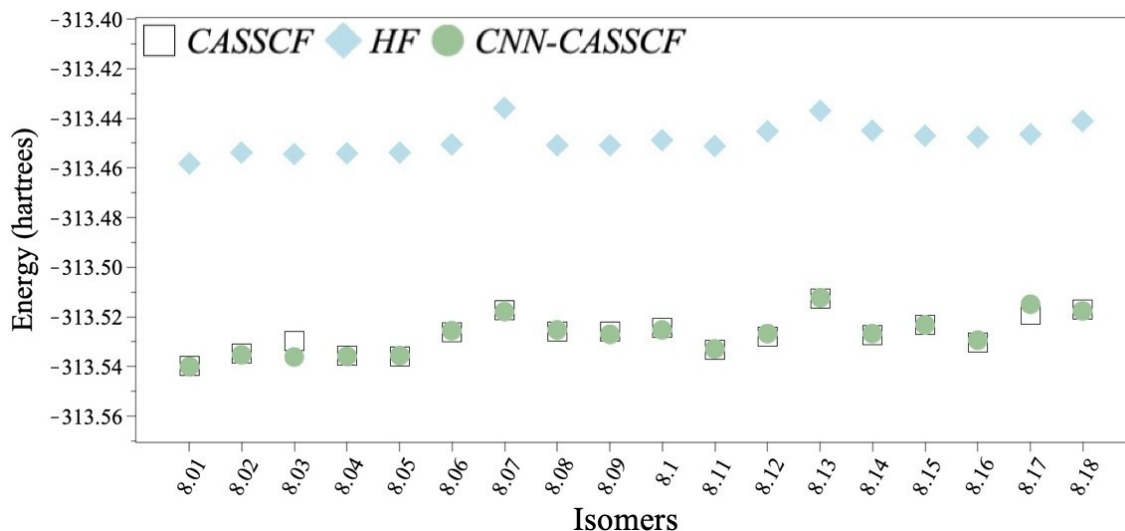
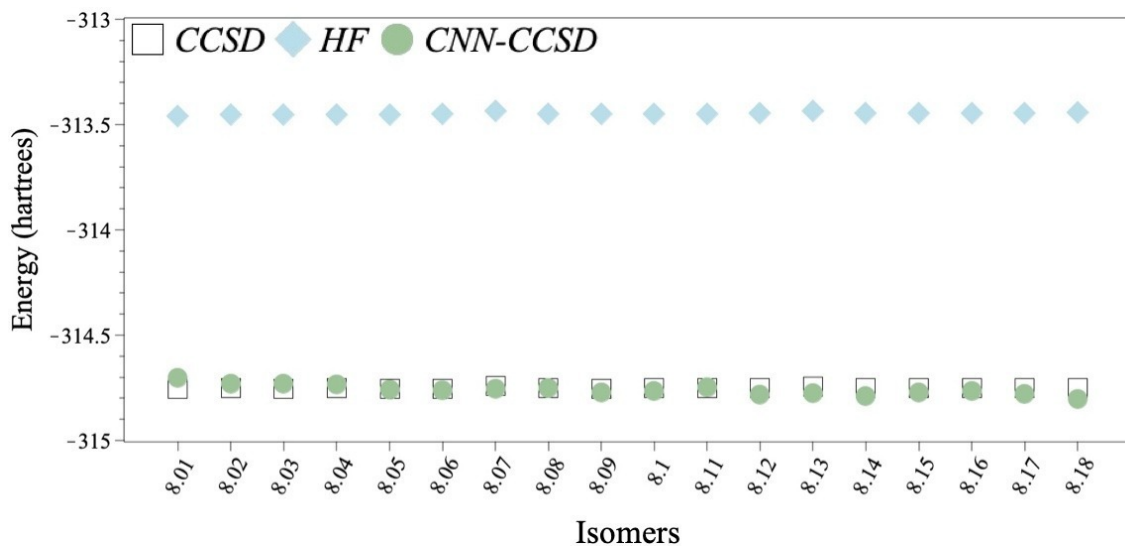
Demonstrating the power of this technique, we train a convolutional neural network on small hydrocarbon systems—with the number of carbon atoms ranging from two to seven—in order to predict CASSCF energies for larger hydrocarbon systems—with the number of carbons ranging from eight to fifteen. We find that our RDM-based machine learning approach accurately recovers the correlation energy for the larger hydrocarbon systems. Thus, our trained convolutional neural network allows us to predict CASSCF-like results at significantly lower computational expense.

While the hydrocarbons involved in training and testing this implementation of our machine-learning reduced density matrix approach do not demonstrate large degrees of correlation, the prediction of accurate correlation energies for larger molecular systems of the type included in the training set likely indicates that as long as the convolutional neural network is trained on appropriate small molecules, the energies of highly-correlated, larger molecules should be able to be obtained via our methodology. Specifically, if one wishes to predict the energy of a molecule which demonstrates a fairly-large degree of correlation, smaller correlated systems would likely be necessary to train the neural network. Application of our machine-learning reduced density matrix approach to highly-correlated systems is a future direction of this research.

This work foreshadows the promise of machine learning in molecular electronic structure calculations, demonstrating that “learning” information about less-expensive, smaller molecular systems can be directly applied to larger typically more-expensive molecules. Future electronic structure methodologies may even include pre-trained convolutional neural networks—possibly varying with the types of atoms, basis set, active space, functional groups, and/or degree of bond saturation inherent to the molecular system of interest—trained on FCI (or similarly expensive) correlation temperatures. This work serves as an initial step in the realization of a combined reduced-density-matrix and machine-learning approach that may provide a real advance in decreasing computational expense for large, highly-correlated electronic structure calculations.

Supporting Information

An analysis of the effect of changing the active space size on our machine-learning reduced density matrix approach; application of our reduced density matrix machine learning algorithm to the prediction of CASSCF energies with a [10,10] active space and cc-pVTZ basis set; application of our reduced density matrix machine learning algorithm to the prediction of CCSD energies with a STO-6G basis.

(a) CASSCF, cc-pVDZ, [$N_e = 8$, $N_o = 8$]

(b) CCSD, cc-pVDZ

FIG. 3: **Octane data.** Hartree-Fock energies (HF, blue diamonds), (a) Complete Active Space Self-Consistent Field/(b) Coupled Cluster Single Double (CASSCF/CCSD, black boxes) energies, and energy values predicted via utilization of Convolutional Neural Networks (CNN, green circles) are shown for the series of octane isomers. As can be seen, the CNN methodology trained on smaller hydrocarbon data fairly accurately recovers the correlation energy. Isomer labels are given by [8.01: ‘Octane’, 8.02: ‘2-Methylheptane’, 8.03: ‘3-Methylheptane’, 8.04: ‘4-Methylheptane’, 8.05: ‘2,2-Dimethylhexane’, 8.06: ‘2,3-Dimethylhexane’, 8.07: ‘2,4-Dimethylhexane’, 8.08: ‘2,5-Dimethylhexane’, 8.09: ‘3,3-Dimethylhexane’, 8.10: ‘3,4-Dimethylhexane’, 8.11: ‘3-Ethylhexane’, 8.12: ‘2,2,3-Trimethylpentane’, 8.13: ‘2,2,4-Trimethylpentane’, 8.14: ‘2,3,3-Trimethylpentane’, 8.15: ‘2,3,4-Trimethylpentane’, 8.16: ‘3-Ethyl-2-Methylpentane’, 8.17: ‘3-Ethyl-3-Methylpentane’, 8.18: ‘2,2,4,4-Tetramethylbutane’]. Hartree-Fock, CASSCF, and CCSD calculations are all computed here using Dunning’s double-zeta (cc-pVDZ) basis set with the CASSCF calculations employing a [$N_e = 8$, $N_o = 8$] active space.

Acknowledgements

D.A.M. gratefully acknowledges support from U.S. National Science Foundation under Grant No. 2155082 and the Department of Energy, Office of Basic Energy Sciences under Grant No. DE-SC0019215. L.M.S.-S. also acknowledges support from the U. S. National Science Foundation under

Grant No. DGE-1746045.

References

* damazz@uchicago.edu

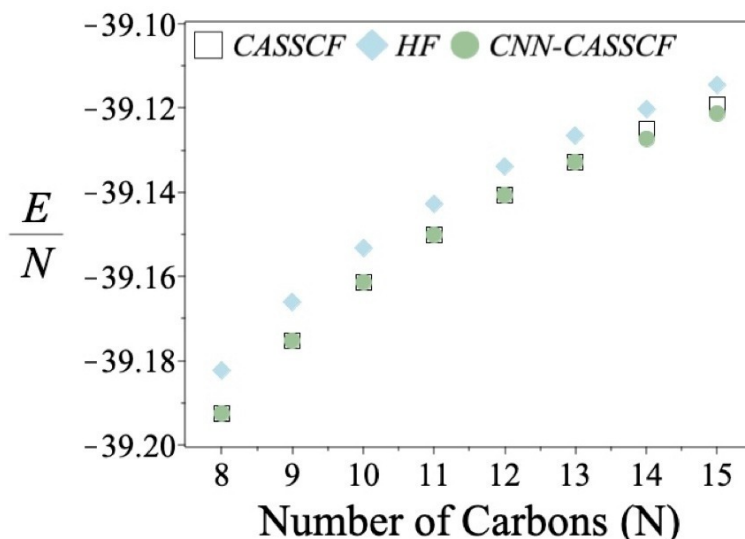


FIG. 4: **Large hydrocarbon data.** Hartree-Fock energies (HF, blue diamonds), Complete Active Space Self-Consistent Field energies (CASSCF, black boxes), and energy values predicted via utilization of Convolutional Neural Networks (CNN, green circles) per number of carbons are shown for the series of straight-chained hydrocarbons from octane through pentadecane. As can be seen, the CNN methodology trained on smaller hydrocarbon data fairly accurately recovers the correlation energy. Isomer labels are given by [8: ‘Octane’, 9: ‘Nonane’, 10: ‘Decane’, 11: ‘Undecane’, 12: ‘Dodecane’, 13: ‘Tridecane’, 14: ‘Tetradecane’, 15: ‘Pentadecane’]. Both Hartree-Fock and CASSCF calculations are computed here using Dunning’s double-zeta (cc-pVDZ) basis set with the CASSCF calculations employing a $[N_e = 8, N_o = 8]$ active space.

- [1] P. J. Knowles and N. C. Handy, Unlimited full configuration interaction calculations, *J. Chem. Phys.* **91**, 2396 (1989).
- [2] F. Jensen, *Introduction to computational chemistry*, 3rd ed. (John Wiley & Sons, Nashville, TN, 2017).
- [3] C. W. Bauschlicher, Jr, S. R. Langhoff, and P. R. Taylor, Accurate quantum chemical calculations, in *Advances in Chemical Physics*, Advances in chemical physics (John Wiley & Sons, Inc., Hoboken, NJ, USA, 2007) pp. 103–161.
- [4] P. G. Mezey, M. G. Papadopoulos, R. Zalesny, and J. Leszczynski, eds., *Linear-scaling techniques in computational chemistry and physics*, 2011th ed., Challenges and Advances in Computational Chemistry and Physics (Springer, Dordrecht, Netherlands, 2011).
- [5] M. Sajjan, J. Li, R. Selvarajan, S. H. Sureshbabu, S. S. Kale, R. Gupta, V. Singh, and S. Kais, Quantum machine learning for chemistry and physics, *Chem. Soc. Rev.* **51**, 6475 (2022).
- [6] S. H. Sureshbabu, M. Sajjan, S. Oh, and S. Kais, Implementation of quantum machine learning for electronic structure calculations of periodic systems on quantum computing devices, *J. Chem. Inf. Model.* **61**, 2667 (2021).
- [7] A. Borin and D. A. Abanin, Approximating power of machine-learning ansatz for quantum many-body states, *Phys. Rev. B* **101**, 195141 (2020).
- [8] Torlai, G, *Augmenting Quantum Mechanics with Artificial Intelligence*, Ph.D. thesis, University of Waterloo, Waterloo, Ontario, Canada (2018).
- [9] K. Ch’ng, J. Carrasquilla, R. G. Melko, and E. Khatami, Machine learning phases of strongly correlated fermions, *Phys. Rev. X* **7**, 031038 (2017).
- [10] F. Brockherde, L. Vogt, L. Li, M. E. Tuckerman, K. Burke, and K.-R. Müller, Bypassing the Kohn-Sham equations with machine learning, *Nat. Commun.* **8**, 872 (2017).
- [11] J. C. Snyder, M. Rupp, K. Hansen, K.-R. Müller, and K. Burke, Finding density functionals with machine learning, *Phys. Rev. Lett.* **108**, 253002 (2012).
- [12] J. Gedeon, J. Schmidt, M. J. P. Hodgson, J. Wetherell, C. L. Benavides-Riveros, and M. A. L. Marques, Machine learning the derivative discontinuity of density-functional theory, *Mach. Learn.: Sci. Technol.* **3**, 015011 (2022).
- [13] K. Mills, M. Spanner, and I. Tamblin, Deep learning and the Schrödinger equation, *Phys. Rev. A* **96**, 042113 (2017).
- [14] X. Wang, A. Kumar, C. R. Shelton, and B. M. Wong, Harnessing deep neural networks to solve inverse problems in quantum dynamics: machine-learned predictions of time-dependent optimal control fields, *Phys. Chem. Chem. Phys.* **22**, 22889 (2020).
- [15] G. Carleo and M. Troyer, Solving the quantum many-body problem with artificial neural networks, *Science* **355**, 602 (2017).
- [16] A. J. Coleman and V. I. Yukalov, *Reduced Density Matrices*, 2000th ed., Lecture Notes in Chemistry (Springer, Berlin, Germany, 2000).
- [17] D. Ter Haar, Theory and applications of the density matrix, *Rep. Prog. Phys.* **24**, 304 (1961).
- [18] D. A. Mazziotti, Pure- N -representability conditions of two-fermion reduced density matrices, *Phys. Rev. A* **94**, 032516 (2016).
- [19] N. Shenvi and A. F. Izmaylov, Active-space N -representability constraints for variational two-particle reduced density matrix calculations, *Phys. Rev. Lett.* **105**, 213003 (2010).
- [20] M. Piris, Global method for electron correlation, *Phys. Rev. Lett.* **119**, 063002 (2017).
- [21] A. J. Coleman, Structure of fermion density matrices, *Rev. Mod. Phys.* **35**, 668 (1963).
- [22] D. A. Mazziotti, ed., *Reduced-density-matrix mechanics*, Advances in Chemical Physics (Wiley-Blackwell, Chichester, England, 2007).

- [23] A. J. Coleman, Structure of fermion density matrices, *Rev. Mod. Phys.* **35**, 668 (1963).
- [24] C. Garrod and J. K. Percus, Reduction of the N-particle variational problem, *J. Math. Phys.* **5**, 1756 (1964).
- [25] R. M. Erdahl, Representability, *Int. J. Quantum Chem.* **13**, 697 (1978).
- [26] R. M. Erdahl, Two algorithms for the lower bound method of reduced density matrix theory, *Rep. math. phys.* **15**, 147 (1979).
- [27] R. Erdahl and V. H. Smith, eds., *Density matrices and density functionals* (Springer, Dordrecht, Netherlands, 2011).
- [28] D. A. Mazziotti, Contracted schrödinger equation: Determining quantum energies and two-particle density matrices without wave functions, *Phys. Rev. A* **57**, 4219 (1998).
- [29] D. A. Mazziotti, Comparison of contracted schrödinger and coupled-cluster theories, *Phys. Rev. A* **60**, 4396 (1999).
- [30] R. M. Erdahl and B. Jin, The lower bound method for reduced density matrices, *Theochem* **527**, 207 (2000).
- [31] M. Nakata, H. Nakatsuji, M. Ehara, M. Fukuda, K. Nakata, and K. Fujisawa, Variational calculations of fermion second-order reduced density matrices by semidefinite programming algorithm, *J. Chem. Phys.* **114**, 8282 (2001).
- [32] D. A. Mazziotti, Variational minimization of atomic and molecular ground-state energies via the two-particle reduced density matrix, *Phys. Rev. A* **65**, 062511 (2002).
- [33] D. A. Mazziotti, Realization of quantum chemistry without wave functions through first-order semidefinite programming, *Phys. Rev. Lett.* **93**, 213001 (2004).
- [34] Z. Zhao, B. J. Braams, M. Fukuda, M. L. Overton, and J. K. Percus, The reduced density matrix method for electronic structure calculations and the role of three-index representability conditions, *J. Chem. Phys.* **120**, 2095 (2004).
- [35] G. Gidofalvi and D. A. Mazziotti, Spin and symmetry adaptation of the variational two-electron reduced-density-matrix method, *Phys. Rev. A* **72**, 052505 (2005).
- [36] D. A. Mazziotti, Quantum chemistry without wave functions: two-electron reduced density matrices, *Acc. Chem. Res.* **39**, 207 (2006).
- [37] D. A. Mazziotti, Anti-hermitian part of the contracted schrödinger equation for the direct calculation of two-electron reduced density matrices, *Phys. Rev. A* **75**, 022505 (2007).
- [38] E. Cancès, G. Stoltz, and M. Lewin, The electronic ground-state energy problem: a new reduced density matrix approach, *J. Chem. Phys.* **125**, 64101 (2006).
- [39] D. A. Mazziotti, Anti-hermitian part of the contracted schrödinger equation for the direct calculation of two-electron reduced density matrices, *Phys. Rev. A* **75**, 022505 (2007).
- [40] R. M. Erdahl, The lower bound method for density matrices and semidefinite programming, in *Reduced-Density-Matrix Mechanics: With Application to Many-Electron Atoms and Molecules*, Advances in chemical physics (John Wiley & Sons, Inc., Hoboken, NJ, USA, 2007) pp. 61–91.
- [41] S. Kais, Entanglement, electron correlation, and density matrices, in *Reduced-Density-Matrix Mechanics: With Application to Many-Electron Atoms and Molecules*, Advances in Chemical Physics (John Wiley & Sons, Inc., Hoboken, NJ, USA, 2007) pp. 493–535.
- [42] G. Gidofalvi and D. A. Mazziotti, Active-space two-electron reduced-density-matrix method: complete active-space calculations without diagonalization of the N-electron hamiltonian, *J. Chem. Phys.* **129**, 134108 (2008).
- [43] D. A. Mazziotti, Parametrization of the two-electron reduced density matrix for its direct calculation without the many-electron wave function, *Phys. Rev. Lett.* **101**, 253002 (2008).
- [44] G. Gidofalvi and D. A. Mazziotti, Direct calculation of excited-state electronic energies and two-electron reduced density matrices from the anti-hermitian contracted schrödinger equation, *Phys. Rev. A* **80**, 022507 (2009).
- [45] J. W. Snyder, Jr, A. E. Rothman, J. J. Foley, 4th, and D. A. Mazziotti, Conical intersections in triplet excited states of methylene from the anti-hermitian contracted schrödinger equation, *J. Chem. Phys.* **132**, 154109 (2010).
- [46] D. A. Mazziotti, Large-scale semidefinite programming for many-electron quantum mechanics, *Phys. Rev. Lett.* **106**, 083001 (2011).
- [47] D. A. Mazziotti, Two-electron reduced density matrix as the basic variable in many-electron quantum chemistry and physics, *Chem. Rev.* **112**, 244 (2012).
- [48] D. A. Mazziotti, Structure of fermionic density matrices: Complete n -representability conditions, *Phys. Rev. Lett.* **108**, 263002 (2012).
- [49] B. Verstichel, H. van Aggelen, W. Poelmans, and D. Van Neck, Variational two-particle density matrix calculation for the Hubbard model below half filling using spin-adapted lifting conditions, *Phys. Rev. Lett.* **108**, 213001 (2012).
- [50] A. M. Sand and D. A. Mazziotti, Enhanced computational efficiency in the direct determination of the two-electron reduced density matrix from the anti-hermitian contracted schrödinger equation with application to ground and excited states of conjugated π -systems, *J. Chem. Phys.* **143**, 134110 (2015).
- [51] W. Poelmans, M. Van Raemdonck, B. Verstichel, S. De Baerdemacker, A. Torre, L. Lain, G. E. Massaccesi, D. R. Alcoba, P. Bultinck, and D. Van Neck, Variational optimization of the second-order density matrix corresponding to a seniority-zero configuration interaction wave function, *J. Chem. Theory Comput.* **11**, 4064 (2015).
- [52] A. W. Schlimgen, C. W. Heaps, and D. A. Mazziotti, Entangled electrons foil synthesis of elusive low-valent vanadium oxo complex, *J. Phys. Chem. Lett.* **7**, 627 (2016).
- [53] D. A. Mazziotti, Enhanced constraints for accurate lower bounds on many-electron quantum energies from variational two-electron reduced density matrix theory, *Phys. Rev. Lett.* **117**, 153001 (2016).
- [54] S. Hemmatiyani, M. Sajjan, A. W. Schlimgen, and D. A. Mazziotti, Excited-state spectra of strongly correlated molecules from a reduced-density-matrix approach, *J. Phys. Chem. Lett.* **9**, 5373 (2018).
- [55] D. R. Alcoba, A. Torre, L. Lain, G. E. Massaccesi, O. B. Oña, E. M. Honoré, W. Poelmans, D. Van Neck, P. Bultinck, and S. De Baerdemacker, Direct variational determination of the two-electron reduced density matrix for doubly occupied-configuration-interaction wave functions: The influence of three-index N-representability conditions, *J. Chem. Phys.* **148**, 024105 (2018).
- [56] J.-N. Boyn, J. Xie, J. S. Anderson, and D. A. Mazziotti, Entangled electrons drive a non-superexchange mechanism in a cobalt quinoid dimer complex, *J. Phys. Chem. Lett.* **11**, 4584 (2020).
- [57] J. Xie, J.-N. Boyn, A. S. Filatov, A. J. McNeece, D. A. Mazziotti, and J. S. Anderson, Redox, transmetalation, and stacking properties of tetrathiafulvalene-2,3,6,7-tetrathiolate bridged tin, nickel, and palladium compounds, *Chem. Sci.* **11**, 1066 (2019).
- [58] J.-N. Boyn and D. A. Mazziotti, Accurate singlet-triplet gaps in biradicals via the spin averaged anti-hermitian contracted schrödinger equation, *J. Chem. Phys.* **154**, 134103 (2021).
- [59] S. Ewing and D. A. Mazziotti, Correlation-driven phenomena in periodic molecular systems from variational two-electron

reduced density matrix theory, *J. Chem. Phys.* **154**, 214106 (2021).

- [60] S. Kim, J. Chen, T. Cheng, A. Gindulyte, J. He, S. He, Q. Li, B. A. Shoemaker, P. A. Thiessen, B. Yu, L. Zaslavsky, J. Zhang, and E. E. Bolton, *PubChem in 2021: new data content and improved web interfaces*, *Nucleic Acids Research* **49**, D1388 (2020), <https://academic.oup.com/nar/article-pdf/49/D1/D1388/35363961/gkaa971.pdf>.
- [61] J. M. Montgomery and D. A. Mazziotti, *Maple’s quantum chemistry package in the chemistry classroom*, *J. Chem. Educ.* **97**, 3658 (2020).
- [62] RDMChem, *Maple Quantum Chemistry Package from RDM-Chem 2022* (Maplesoft, Waterloo, Ontario, 2022).
- [63] Maplesoft, *Maple 2022* (Maplesoft, Waterloo, Ontario, 2022).
- [64] F. Chollet, *Keras 2015* (GitHub, San Francisco, CA, 2015).

Experimental

Computational Methods. The molecular geometries for all hydrocarbon isomers are obtained from the PubChem database [60]. Molecular energies are then computed for Hartree-Fock, Complete Active Space Self-Consistent Field (CASSCF), and Coupled Cluster Single Double (CCSD) levels of theory through use of a Dunning’s double-zeta (cc-pVDZ) basis set, with the CASSCF calculations employing a [$N_e = 8$, $N_o = 8$] active space. These calculations are accomplished via the Quantum Chemistry Toolbox [61, 62] in the Maple computing environment [63]. Note that while—throughout this text—the size of the active space for the training and testing molecules is made identically [$N_e = 8$, $N_o = 8$] for all CASSCF calculations, changing active space sizes with the number of carbons yielded similar results to those we present here. (See the Supporting Information for additional details.)

Computation of Geminal Energies and Populations. The reduced Hamiltonian (2K) shown in Eq. (2) is obtained by directly computing the one electron integrals and the electron repulsion integrals via the MOIntegrals function of the Quantum Chemistry Toolbox [61] in the Maple computing environment [63] and then applying the appropriate conversions to put it into the same orbital basis as the 2-RDM. The geminal energies (ϵ_i) then correspond to the eigenvalues of the 2K matrix. The populations (p_i) of the geminals are then obtained via the following

$$p_i = \langle v_i | {}^2D | v_i \rangle \quad (6)$$

where v_i is the eigenvector of the reduced Hamiltonian corresponding to the the geminal energy ϵ_i and where 2D is the particle-particle reduced density matrix (2-RDM).

Convolutional Neural Network.

Model Inputs. For a given molecular system, both the geminal energies (ϵ_i) and the Hartree-Fock correlation temperature (T_{HF}^*) are input into the convolutional neural network. Specifically, the geminal energies are encoded as partition functions (Z)—computed according to Eq. (5)—for β val-

ues ranging from 0 to 20 by 0.4 where

$$\beta = \frac{1}{kT} \quad (7)$$

and where k is the Boltzmann constant. The Hartree-Fock correlation temperature is obtained by inserting Eq. (5) into Eq. (4) which is inserted into Eq. (3) to obtain

$$E(T) = \frac{N(N-1)}{\sum_i e^{i\epsilon_i/kT}} \sum_j \epsilon_j e^{-\epsilon_j/kT} \quad (8)$$

and then temperature is optimized via `scipy.optimize.minimize` such that $|E_{HF} - E(T)|$ is minimized.

Model Outputs. For a given molecular system, the output of the convolutional neural net is a Δ value representing the difference between the Hartree-Fock correlation temperature and the predicted CASSCF correlation temperature, i.e., $\Delta = T_{CAS}^* - T_{HF}^*$. From this output, the predicted correlation temperature corresponding to the CASSCF calculation can be computed by adding the output (Δ) to the Hartree-Fock correlation temperature (T_{HF}^*), which can be used—along with the known geminal energies (ϵ_i)—to calculate the predicted CASSCF energy according to Eq. (8).

Training Data. All hydrocarbons isomers ranging from two to seven carbon atoms are used to train the convolutional neural net. Specifically, the training set—composed of twenty-one hydrocarbon molecules—follows: 2.01: ‘Ethane’, 3.01: ‘Propane’, 4.01: ‘Butane’, 4.02: ‘2-Methylpropane’, 5.01: ‘Pentane’, 5.02: ‘2-Methylbutane’, 5.03: ‘2,2-Dimethylpropane’, 6.01: ‘Hexane’, 6.02: ‘2-Methylpentane’, 6.03: ‘3-Methylpentane’, 6.04: ‘2,2-Dimethylbutane’, 6.05: ‘2,3-Dimethylbutane’, 7.01: ‘Heptane’, 7.02: ‘3-Methylhexane’, 7.03: ‘2-Methylhexane’, 7.04: ‘2,2-Dimethylpentane’, 7.05: ‘2,3-Dimethylpentane’, 7.06: ‘2,4-Dimethylpentane’, 7.07: ‘3,3-Dimethylpentane’, 7.08: ‘3-Ethylpentane’, 7.09: ‘2,2,3-Trimethylbutane’.

Testing Data. All isomers of octane isomers as well as nonane, decane, undecane, dodecane, tridecane, tetradecane, and pentadecane are used to test the trained neural net. Specifically, the testing set follows: 8.01: ‘Octane’, 8.02: ‘2-Methylheptane’, 8.03: ‘3-Methylheptane’, 8.04: ‘4-Methylheptane’, 8.05: ‘2,2-Dimethylhexane’, 8.06: ‘2,3-Dimethylhexane’, 8.07: ‘2,4-Dimethylhexane’, 8.08: ‘2,5-Dimethylhexane’, 8.09: ‘3,3-Dimethylhexane’, 8.1: ‘3,4-Dimethylhexane’, 8.11: ‘3-Ethylhexane’, 8.12: ‘2,2,3-Trimethylpentane’, 8.13: ‘2,2,4-Trimethylpentane’, 8.14: ‘2,3,3-Trimethylpentane’, 8.15: ‘2,3,4-Trimethylpentane’, 8.16: ‘3-Ethyl-2-Methylpentane’, 8.17: ‘3-Ethyl-3-Methylpentane’, 8.18: ‘2,2,4,4-Tetramethylbutane’, 9.01: ‘Nonane’, 10.01: ‘Decane’, 11.01: ‘Undecane’, 12.01: ‘Dodecane’, 13.01: ‘Tridecane’, 14.01: ‘Tetradecane’, 15.01: ‘Pentadecane’.

CNN Specifics. The convolutional neural network is composed of an input layer, five additional dense layers, and an

output layer. The input layer consists of partition functions and the Hartree-Fock correlation temperature as specified in the *Model Inputs* section, and the output layer is a dense layer consisting of the Δ value described in the *Model Outputs* section. The additional dense layers have 503, 240, 100, 50, and 20 nodes, respectively. All dense nodes are initialized via the *he_uniform* kernel initializer with a *relu* activation function. For the training of the convolutional net, loss is measured via mean absolute error, and the *adam* optimizer is implemented for 30,000 epochs. This convolutional neural network is implemented using Keras—Python’s deep learning API [64].

Computational Scaling

For the testing set, scaling is dominated by the determination of the geminal energies, which are obtained via the diagonalization of the two-electron reduced Hamiltonian, a computation that scales as $O[r^6]$ where r is the number of orbitals in the active space. Thus, for a given molecule in the testing set, computational expense for prediction of molecular energies scales as $O[r^6]$. The computational expense of the training set is dominated by the determination of the reference CASSCF or CCSD energies necessary to obtain

the reference correlation temperature—which are known to scale approximately as $O[N!]$ and $O[N^6]$, respectively, for a given molecule where N for CASSCF is the number of active electrons and N for CCSD is the number of total electrons.

TOC Graphic

